

Cryogenic Subthreshold Swing Saturation in FD-SOI MOSFETs described with Band Broadening

H. Bohuslavskyi, A. G. M. Jansen, S. Barraud, V. Barral, M. Cassé, L. Le Guevel, X. Jehl, L. Hutin, B. Bertrand, G. Billiot, G. Pillonnet, F. Arnaud, P. Galy, S. De Franceschi, M. Vinet, and M. Sanquer

arXiv:1903.05409v1 [cond-mat.mes-hall] 13 Mar 2019

Abstract—In the standard MOSFET description of the drain current I_D as a function of applied gate voltage V_{GS} , the subthreshold swing $SS(T) \equiv dV_{GS}/d \log I_D$ has a fundamental lower limit as a function of temperature T given by $SS(T) = \ln 10 k_B T/e$. However, recent low-temperature studies of different advanced CMOS technologies have reported $SS(4\text{ K or lower})$ values that are at least an order of magnitude larger. Here, we present and analyze the saturation of $SS(T)$ in 28 nm fully-depleted silicon-on-insulator (FD-SOI) devices for both n- and p-type MOSFETs of different gate oxide thicknesses and gate lengths down to 4 K. Until now, the increase of interface-trap density close to the band edge as temperature decreases has been put forward to understand the saturation. Here, an original explanation of the phenomenon is presented by considering a disorder-induced tail in the density of states at the conduction (valence) band edge for the calculation of the MOS channel transport by applying Fermi-Dirac statistics. This results in a subthreshold $I_D \sim e^{eV_{GS}/k_B T_0}$ for $T_0 = 35\text{ K}$ with saturation value $SS(T < T_0) = \ln 10 k_B T_0/e$. The proposed model adequately describes the experimental data of $SS(T)$ from 300 down to 4 K using $k_B T_0 \simeq 3\text{ meV}$ for the width of the exponential tail and can also accurately describe $SS(I_D)$ within the whole subthreshold region. Our analysis allows a direct determination of the technology-dependent band-tail extension forming a crucial element in future compact modeling and design of cryogenic circuits.

Index Terms—Cryogenic electronics, MOSFET, Subthreshold Swing, 28nm FD-SOI, Band tail, Quantum computing.

I. INTRODUCTION

The development of electronic circuits at cryogenic temperatures (4 K or even lower) has great importance for a large spectrum of applications such as high-performance classical computing, cryogenic sensors and detectors, space electronics, low power neuromorphic circuits, and quantum computing [1]–[4]. The nowadays progress in the realization of quantum bit (qubit) systems at low temperatures has proven the necessity of having nearby cryogenic electronics to enable fast and efficiently-controlled manipulation and read-out of a large number of qubits [1], [5], [6]. In this respect, the recent demonstrations of silicon qubits could be combined with state-of-the-art CMOS electronics [7]–[9].

This work was supported by the EU Research and Innovation program Horizon 2020 under grant agreement No 688539 MOSQUITO.

H. Bohuslavskyi, S. Barraud, V. Barral, M. Cassé, L. Le Guevel, L. Hutin, B. Bertrand, G. Billiot, G. Pillonnet, and M. Vinet are with CEA, LETI, MINATEC Campus, F-38054 Grenoble, France.

A. G. M. Jansen, X. Jehl, S. De Franceschi, and M. Sanquer are with Univ. Grenoble Alpes, CEA, INAC-PHELIQS, F-38054 Grenoble, France.

F. Arnaud and P. Galy are with STMicroelectronics, 850 rue J. Monnet, 38920 Crolles, France.

Corresponding authors: marc.sanquer@cea.fr and louis.jansen@cea.fr

The 28nm fully-depleted silicon-on-insulator (FD-SOI) MOSFETs with undoped channel have numerous advantages for low-temperature applications compared to Si bulk transistors, such as the reduced impact of dopant freeze-out, reduced variability, tuning of threshold voltage thanks to back-biasing, higher mobility, and quasi-ideal electrostatic control [10], [11].

The present study focuses on the exponential gate-voltage (V_{GS}) dependence of the subthreshold drain current I_D of a MOSFET as a function of the temperature T captured by the subthreshold swing $SS(T) \equiv dV_{GS}/d \log I_D = m \ln 10 k_B T/e$ [12] ($SS(300\text{ K}) = 60\text{ mV/dec}$ for $m = 1$), where k_B is the Boltzmann constant and e the absolute elementary charge. The factor $m = (C_{ox} + C_{it})/C_{ox} \geq 1$ takes into account the capacitance of the interface traps C_{it} with respect to the geometric gate capacitance C_{ox} (in our case of FD-SOI, the depletion capacitance can be neglected). The very small value of SS in the (sub)K-range results in an ideal $I_D(V_{GS})$ switch leading to a high on/off current ratio and low power dissipation in the stand-by regime.

Cryogenic investigations of $SS(T)$ in advanced CMOS devices reveal at least one order of magnitude larger values at 4 K compared with the expected value $SS(4\text{ K}) = 0.79\text{ mV/dec}$ for $m = 1$. For bulk MOSFETs, typical values for $SS(4\text{ K})$ range from 30 to 10 mV/dec [3], [4], [13], [14]. Even though an effective operation of different SOI technologies at cryogenic temperature has been demonstrated, the reported SS values turned out to be as high as 7 mV/dec at 4K [15]–[18], even at sub-1K temperatures [19].

Common explanations correlate the $SS(T)$ dependence in bulk Si transistors to an important increase of the density of interface traps D_{it} close to the band edges [20]. Similarly, for planar SOI devices, the increase of D_{it} has been demonstrated to extend more than 100 meV inside the band gap using the spectroscopic charge-pumping technique [21]. However, especially at the lowest temperatures, analyzing the saturation with a strongly temperature dependent increase of m via $C_{it} = e^2 D_{it}$ leads to an estimate of unrealistic D_{it} values that are even larger than the silicon density of states of free carriers [19]. More recently, a constant contribution to $SS(T)$ has been derived at 4 K by modeling the thermal occupation of the interface-trap distribution [17], [22]–[24] which needs temperature-specific modeling for an application to all temperatures.

In order to explain the cryogenic saturation of SS , we propose a new approach introducing a disorder-induced exponential tail in the density of states (DOS) for the calculation of the subthreshold charge-carrier transport. The model is

validated on the experimental data of long- and short-channel MOSFETs with different oxide thicknesses in terms of both $SS(T)$ and $SS(I_D)$ dependences from 300 K down to 4.3 K.

II. EXPERIMENT

Thin (GO1) and thick (GO2) gate oxide low-threshold-voltage (LVT) FD-SOI transistors were fabricated with a gate-first high- κ metal gate by STMicroelectronics on 300 mm (100) SOI wafers with a buried oxide thickness of 25 nm [11], [25]. The equivalent oxide thickness (EOT) is 1.55 nm for GO1 and 3.7 nm for GO2. The 7 nm-thick channel is undoped.

Both n-type and p-type long-channel GO2 (gate length $L = 0.15, 2 \mu\text{m}$ and width $W = 2 \mu\text{m}$) and n-type short-channel GO1 ($L = 28, 34 \text{ nm}$ and $W = 80, 210 \text{ nm}$) transistors were investigated. P-type short-channel devices couldn't be analyzed for the $SS(T)$ -dependence because of oscillatory variations in $SS(I_D)$ below threshold at cryogenic temperatures. This results from the enhanced boron diffusion from the source/drain regions affecting subthreshold current at low V_{DS} (see [18], [26]).

The transistors cleaved from a wafer were mounted to the sample holder of a cryogenic probe station equipped with 4 adjustable contact needles connected to Source/Measurement Units. Then, they were cooled down under continuous He flow with temperature regulation between 4 and 300 K. The data acquisition was done using a parameter analyzer (HP 4155A).

Fig. 1a shows $I_D(V_{GS})$ at temperatures between 300 and 4.3 K for the n-type long- and short-channel devices at $|V_{DS}| = 50 \text{ mV}$ and back-gate voltage $V_{BACK} = 0 \text{ V}$. Both cases reveal a classical, oscillation-free $I_D(V_{GS})$ down to the lowest temperatures. The saturation of $SS(T)$ below about 40 K can be clearly seen from the $SS(I_D)$ data as illustrated in Fig. 1b. The same trend holds for p-type long-channel and n-type short-channel devices.

In Fig. 1c, $SS(T)$ from 300 K down to roughly 40 K follows the expected dependence $m_{1,2} \ln 10 k_B T/e$ with $m_1 = 1.14$ for the long devices and $m_2 = 1.23$ for the short device. The slightly higher SS (described by $m_1 = 1.14$) for the long devices is explained by the presence of interface traps (C_{it}), and the larger $m_2 = 1.23$ follows from additional electrostatic short-channel effects [27]. $SS(4.3 \text{ K})$ saturates at 7.3 mV/dec for n-type long-channel, 7.4 mV/dec for p-type long-channel, and 7.7 mV/dec for n-type short-channel.

III. MODEL DESCRIPTION AND DISCUSSION

The diffusive subthreshold transport is proportional to the density n of the mobile charge carriers in the channel assuming a constant diffusion constant (mobility) [12]. Using the Fermi-Dirac statistics for the occupation of electron states [27], [28], here for the n-type case, n can be expressed as a function of the semiconductor potential Ψ_s via

$$n(\Psi_s) = \int_{-\infty}^{\infty} f(E) N_c^{2D}(E) dE, \quad (1)$$

with the Fermi function $f(E) = 1/(e^{(E-E_c)/k_B T} + 1)$ and a step function for the two-dimensional DOS $N_c^{2D}(E)$ from zero to $N_c^{2D} = g_v m^*/\pi \hbar^2$ at the band edge $E_c = E_c^0 - e\Psi_s$.

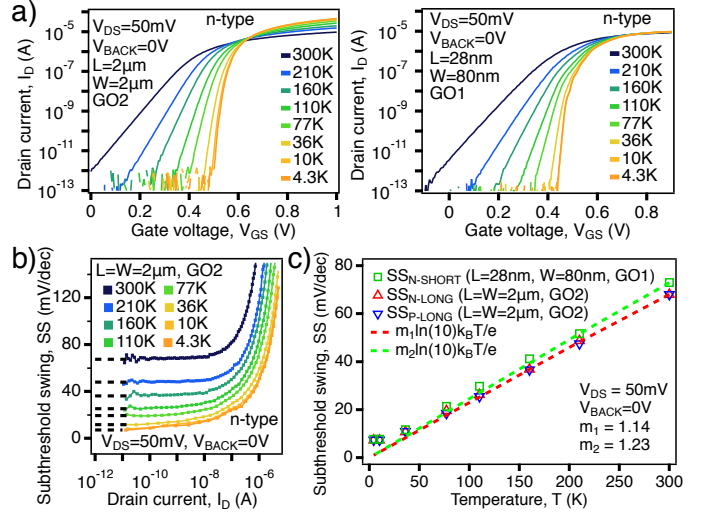


Fig. 1. a) $I_D(V_{GS})$ characteristics at different temperatures recorded at $V_{DS} = 50 \text{ mV}$. Left and right panel show the case of n-type long- and short-channel MOSFETs. b) $SS(I_D)$ for the n-type long-channel. c) $SS(T)$ obtained by extrapolating SS at $I_D = 10^{-11} \text{ A}$ for n- and p-type long-channel ($SS_{N,P-LONG}$) and n-type short-channel ($SS_{N-SHORT}$) transistors. Dashed lines stand for the expected linear temperature dependence $m_{1,2} \ln 10 k_B T/e$ with $m_1 = 1.14$ and $m_2 = 1.23$.

For the flat band condition with $\Psi_s = 0$, the Fermi energy E_F is taken at mid-gap with $E_c^0 = 0.55 \text{ eV}$ (considering a temperature-independent energy gap 1.1 eV for Si). Other parameters are the valley degeneracy $g_v = 2$ and the effective mass $m^* = 0.19 m_0$ (free-electron mass m_0). Finally, the equilibrium electron density $n(\Psi_s)$ can be transposed to $n(V_{GS})$ using $V_{GS} = \Psi_s + n(\Psi_s)e/C_{ox}$ [27], for the sum of the semiconductor potential Ψ_s and the voltage drop ne/C_{ox} over the geometric gate capacitance $C_{ox} = k\epsilon_0/t_{EOT} [\text{F/m}^2]$ supposing $m = 1$. ϵ_0 is the free-space permittivity, $k = 3.9$ the relative dielectric constant of SiO_2 , and $t_{EOT} = 3.7 \text{ nm}$ the equivalent oxide thickness in case of GO2.

The calculated $n(V_{GS})$ data for a sharp band edge reveal the standard exponential dependence $I_D \sim e^{eV_{GS}/k_B T}$, confirming the linear temperature dependence $SS(T) = \ln 10 k_B T/e$. However, only using the Fermi-Dirac statistics is not enough to explain the experimentally observed saturation at low temperatures as shown in Fig. 1c.

To describe the saturation of SS at low temperatures, a broadened band edge [29], [30] was added to the DOS in the form $N_c^{2D} e^{(E-E_c)/k_B T_0}$ for $E < E_c$ (inset in Fig. 2c). The parameter $k_B T_0$ quantifies the extent of the exponential tail resulting from, e.g., crystalline disorder, residual impurities, and strain, surface roughness, etc. Assuming a proportionality between $I_D(V_{GS})$ and $n(V_{GS})$, the calculated $I_D(V_{GS})$ is shown in Fig. 2a for different temperatures with $T_0 = 35 \text{ K}$ (resulting in $k_B T_0 = 3 \text{ meV}$). A saturation value $SS(T \leq T_0) = \ln 10 k_B T_0/e = 6.9 \text{ mV/dec}$ is obtained for $m = 1$ (see Fig. 2b). The 3 meV tail was determined empirically to describe the experimental $SS(4.3 \text{ K})$ of 7-8 mV/dec.

To compare with the model, the saturation values $SS(T)$ in the weak inversion measured at $I_D = 10 \text{ pA}$ are plotted in Fig. 2c after normalization with the corresponding $m_{1,2}$ (for the values, see Fig. 1c). It should be noted that the chosen

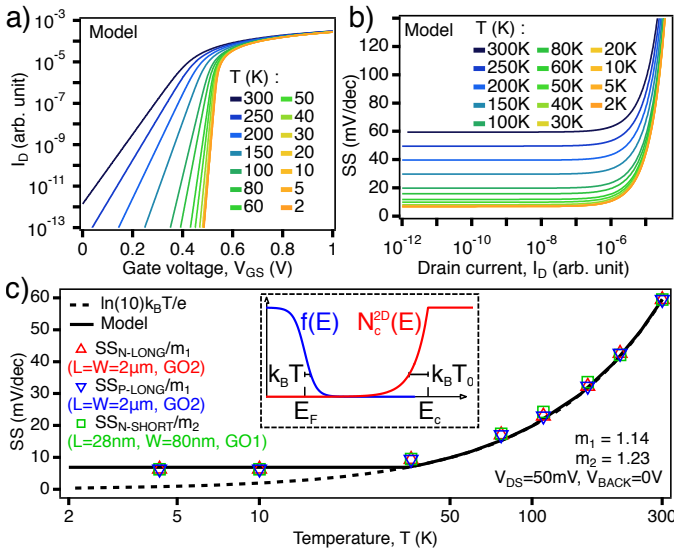


Fig. 2. a) Calculated $I_D(V_{GS})$ for the model parameters given in the main text, assuming an exponential tail below the conduction band edge with $k_B T_0 = 3$ meV. b) Calculated $SS(I_D)$. c) Calculated $SS(T)$ compared to experimental data normalized by $m_{1,2}$ (symbols) and to $\ln(10) k_B T/e$. The inset shows a schematic representation of the exponential tails of the Fermi distribution function $f(E)$ for $E > E_F$ and of the DOS $N_c^{2D}(E)$ for $E < E_c$. The product of $f(E)$ and $N_c^{2D}(E)$ for $T < T_0$ gives the distribution of occupied states with a maximum around E_F .

$k_B T_0$ gives a good description of the experimental data for all studied MOSFETs. The obtained exponential extent for the band tail is comparable to that of 2-10 meV probed with Electron Spin Resonance on Si MOSFETs in [31].

FD-SOI cryogenic back-biasing was already demonstrated to be efficient down to 4 K [32]. By using forward back-biasing (FBB), the conductive channel can be displaced towards the Si-BOX interface. Therefore, if the increase of D_{it} was responsible for $SS(T)$ saturation, one would expect a significant difference in $SS(I_D)$ profiles. However, the experimental data in Fig. 3a and 3b for an n-type device at 4.3 K reveal that $SS(I_D)$ curves hardly change for V_{BACK} up to 3 V, implying that the edge-broadened DOS cannot be explained with just D_{it} at the Si-SiO₂ interface.

At the lowest temperatures, the measured $SS(I_D)$ characteristics reveal an increased gate-voltage dependence (Fig. 1b) as compared to the constant $SS(I_D)$ from our calculations (Fig. 2b). This variation of $SS(I_D)$ can also be modeled by including an energy dependence $m(E)$ in the relation $V_{GS}(\Psi_s) = m(\Psi_s)\Psi_s + n(\Psi_s)e/C_{ox}$, similarly to the description of the interface traps below the band edge with the additional capacitance C_{it} in the introduction. In Fig. 3c the calculated $SS(I_D)$ is shown for an exponential dependence $m(E) \sim e^{(E-E_c)/E_m}$. A good agreement with the experimental data is found for a variation of $m(E)$ from 1.14 to 1.34 with an empirically-determined energy range $E_m = 10$ meV below E_c . Regarding the physical reasoning behind the improved model which includes $m(E)$, we note that not all the states in the band tail contribute to the transport [33]. Therefore, the V_{GS} -induced occupation of states in the band tail influences both the subthreshold current due to mobile states and the efficiency of gate control via $m(\Psi)$ because of trapped states. In

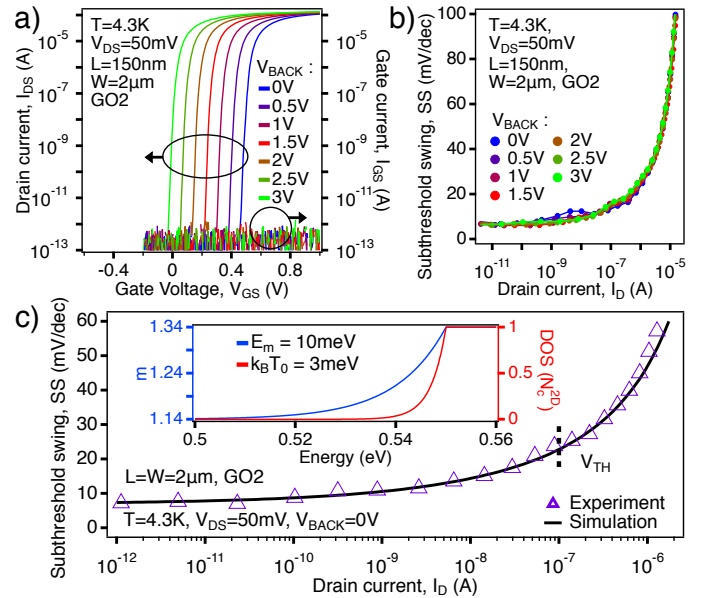


Fig. 3. a) $I_D(V_{GS})$ and $I_G(V_{GS})$ for different V_{BACK} and b) extracted $SS(I_D)$ for the same device at $T = 4.3$ K. Almost the same $SS(I_D)$ profile is observed when the conductive channel is pulled towards the Si-BOX interface under FBB. c) $SS(I_D)$ profile with SS ranging from 7.4 mV/dec ($I_D = 1$ pA) to 23 mV/dec at V_{TH} ($I_D = 0.1$ μ A) for a long-channel n-type device illustrating the increased $SS(V_{GS})$ dependence at $T = 4.3$ K. Accounting for the exponential energy-dependent $m(E)$ and $k_B T_0 = 3$ meV (as shown in the inset), the refined model accurately reproduces the experimental $SS(I_D)$ within the whole subthreshold region in addition to the $SS(T)$ dependence from 300 down to 4.3 K (see Fig. 2c).

our modeling, each of these contributions has its characteristic extent in energy below E_c .

IV. CONCLUSION

To explain the generally observed saturation of SS at low temperature in FD-SOI MOSFETs, an exponential tail at the band edge is introduced yielding $I_D(V_{GS})$ of the form $e^{eV_{GS}/k_B T_0}$ that replaces the usual temperature dependence $e^{eV_{GS}/k_B T}$ for $T < T_0$. The determined $T_0 = 35$ K holds for all measured FD-SOI devices with long- and short-channel lengths for different oxide thickness and accurately describe the $SS(T)$ from 300 K down to 4.3 K. In addition, we address the problem of the increased cryogenic $SS(V_{GS})$ dependence at low temperatures and successfully model a non-constant $SS(I_D)$ profile below V_{TH} by introducing an energy-dependent $m(E)$ in the gate-control efficiency. Finally, our results indicate that the implementation of band-tail broadening could form an important technological parameter for the correct modeling of MOSFETs at low temperatures.

REFERENCES

- [1] D. J. Reilly, "Engineering the quantum-classical interface of solid-state qubits", *Npj Quantum Information*, vol. 1, no. 15011, Oct. 2015. doi: 10.1038/npjqi.2015.11
- [2] M. L. Schneider, C. A. Donnelly, S. E. Russek, B. Baek, M. R. Pufall, P. F. Hopkins, P. D. Dresselhaus, S. P. Benz, and W. H. Rippard, "Ultralow power artificial synapses using nanotextured magnetic Josephson junctions", *Science Advances*, vol. 4, no. 1, Jan. 2018. doi: 10.1126/sciadv.1701329

- [3] E. Gutierrez-D, J. Deen, and C. Claeys, *Low Temperature Electronics: Physics, Devices, Circuits, and Applications*, San Diego, Academic Press, Oct. 2001, pp. 135 - 240.
- [4] H. Homulle, L. Song, E. Charbon, and F. Sebastian, "The Cryogenic Temperature Behavior of Bipolar, MOS, and DTMOS Transistors in Standard CMOS", *IEEE Journal of the Electron Devices Society*, vol. 6, pp. 263-270, 2018. doi: 10.1109/JEDS.2018.279821
- [5] B. Patra, R.M. Incandela, J. P. G. van Dijk, H. A. R. Homulle, L. Song, M. Shahmohammadi, R. B. Staszewski, A. Vladimirescu, M. Babaie, F. Sebastian, and E. Charbon, "Cryo-CMOS Circuits and Systems for Quantum Computing Applications", *IEEE Journal of Solid-State Circuits*, vol. 53, pp. 309-321, 2018. doi: 10.1109/JSSC.2017.2737549
- [6] L. M. K. Vandersypen, H. Bluhm, J. S. Clarke, A. S. Dzurak, R. Ishiihara, A. Morello, D. J. Reilly, L. R. Schreiber, and M. Veldhorst, "Interfacing spin qubits in quantum dots and donors - hot, dense, and coherent", *Npj Quantum Information*, vol. 3, no. 34, Sept. 2017. doi: 10.1038/s41534-017-0038-y15011
- [7] J. T. Muhonen, J. P. Dehollain, A. Laucht, F. E. Hudson, R. Kalra, T. Sekiguchi, K. M. Itoh, D. N. Jamieson, J. C. McCallum, A. S. Dzurak, and A. Morello, "Storing quantum information for 30 seconds in a nanoelectronic device" *Nature Nanotechnology*, vol. 9, pp. 986 - 981, Sept. 2014. doi: 10.1038/NNANO.2014.211
- [8] M. Veldhorst, C. H. Yang, J. C. C. Hwang, W. Huang, J. P. Dehollain, J. T. Muhonen, S. Simmons, A. Laucht, F. E. Hudson, K. M. Itoh, A. Morello, and A. S. Dzurak, "A two-qubit logic gate in silicon", *Nature*, vol. 526, pp. 410 - 414, Oct. 2015. doi: 10.1038/nature15263
- [9] R. Maurand, X. Jehl, D. Kotekar-Patil, A. Corra, H. Bohuslavskyi, R. Lavieille, L. Hutin, S. Barraud, M. Vinet, M. Sanquer, and S. De Franceschi, "A CMOS silicon spin qubit", *Nature Communications*, vol. 7, no. 13575, Oct. 2016. doi: 10.1038/ncomms13575
- [10] B. Doris, B. De Salvo, K. Cheng, P. Morin, and M. Vinet, "Planar Fully-Depleted-Silicon-On-Insulator technologies: Toward the 28nm node and beyond", *Solid-State Electronics*, vol. 117, pp. 37-59, Mar. 2016. doi: 10.1016/j.sse.2015.11.006
- [11] D. Jacquet, F. Hasbani, P. Flatresse, R. Wilson, F. Arnaud, G. Cesana, T. Di Gilio, C. Lecocq, T. Roy, A. Chhabra, C. Grover, O. Minez, J. Uginet, G. Durieu, C. Adobati, D. Casalotto, F. Nyer, P. Menut, A. Cathelin, I. Vongsavady, and P. Magarshack, "A 3 GHz dual core processor ARM Cortex TM -A9 in 28 nm UTBB FD-SOI CMOS with ultra-wide voltage range and energy efficiency optimization", *IEEE Journal of Solid-State Circuits*, vol. 49, pp. 812 - 826, Jan. 2014. doi: 10.1109/JSSC.2013.2295977
- [12] S. M. Sze, *Physics of semiconductor devices (2nd Edition)*, New York, John Wiley & Sons, 1981, pp. 431 - 511.
- [13] H. Hanamura, M. Aoki, T. Masuhara, O. Minato, Y. Sakai, and T. Hayashida, "Operation of bulk CMOS devices at very low temperatures", *IEEE Journal of Solid-State Circuits* vol. 21, no. 3, pp. 484 - 490, Jun. 1986. doi: 10.1109/JSSC.1986.1052555
- [14] R. M. Incandela, L. Song, H. A. R. Homulle, F. Sebastian, E. Charbon, and A. Vladimirescu, "Nanometer CMOS characterization and compact modelling at deep-cryogenic temperatures", *2017 47th European Solid-State Device Research Conference (ESSDERC)*, Leuven, 2017, pp. 58 - 61. doi: 10.1109/ESSDERC.2017.8066591
- [15] B. Roche, B. Voisin, X. Jehl, R. Wacquez, M. Sanquer, M. Vinet, V. Deshpande, and B. Previtali, "A tunable, dual mode field-effect or single electron transistor", *Applied Physics Letters*, vol. 100, no. 032107, Aug. 2012. doi: 10.1063/1.3678042
- [16] M. Shin, M. Shi, M. Mouis, A. Cros, E. Josse, G. T. Kim, and G. Ghibaudo, "Low temperature characterization of 14nm FDSOI CMOS devices", *2014 11th International Workshop on Low Temperature Electronics (WOLTE)*, Grenoble, 2014, pp. 29 - 32. doi: 10.1109/WOLTE.2014.6881018
- [17] A. Beckers, F. Jazaeri, H. Bohuslavskyi, L. Hutin, S. De Franceschi, and C. Enz, "Design-oriented modeling of 28 nm FDSOI CMOS technology down to 4.2K for quantum computing" *2018 Joint International EUROSOI Workshop and International Conference on Ultimate Integration on Silicon (EUROSOI-ULIS)*, Granada, 2018, pp. 1 - 4. doi: 10.1109/ULIS.2018.8354742
- [18] H. Bohuslavskyi, S. Barraud, M. Cassé, V. Barra, B. Bertrand, L. Hutin, F. Arnaud, P. Galy, M. Sanquer, S. De Franceschi, and M. Vinet, 28nm Fully-Depleted SOI Technology: "Cryogenic Control Electronics for Quantum Computing", *2017 Silicon Nanoelectronics Workshop*, Kyoto, 2017, pp. 143-144. doi: 10.23919/SNW.2017.8242338
- [19] P. Galy, J. Camirand Lemyre, P. Lemieux, F. Arnaud, D. Drouin, and M. Pioro-Ladrière, "Cryogenic temperature characterization of a 28-nm FD-SOI dedicated structure for advanced CMOS and quantum technologies co-integration" *IEEE Journal of the Electron Devices Society*, vol. 6, pp. 594 - 600, May 2018. doi: 10.1109/JEDS.2018.2828465
- [20] I. M. Hafez, G. Ghibaudo, and F. Balestra, "Assessment of interface state density in silicon MOS transistors at room, liquid nitrogen, and liquid helium temperatures" *Journal of Applied Physics*, vol. 4, no. 4, pp. 1950 - 1952, Oct. 1990. doi: 10.1063/1.345572
- [21] M. Cassé, K. Tachi, S. Thiele, and T. Ernst, "Spectroscopic charge pumping in Si nanowire transistors with a high- κ /metal gate", *Applied Physics Letters*, vol. 96, no. 123506, Mar. 2010. doi: 10.1063/1.3368122
- [22] A. Beckers, F. Jazaeri, and C. Enz, "Cryogenic MOS transistor model", *IEEE Transactions Electron Devices*, vol. 65, pp. 3617 - 3625, Aug. 2018. doi: 10.1109/TED.2018.2854701
- [23] A. Beckers, F. Jazaeri and C. Enz, "Characterization and modeling of 28-nm Bulk CMOS Technology Down to 4.2 K" *IEEE Journal of the Electron Devices Society*, vol. 6, pp. 1007-1018, Mar. 2018. doi: 10.1109/JEDS.2018.2817458
- [24] A. Beckers, F. Jazaeri and C. Enz, "Revised theoretical limit of the sub-threshold swing in field-effect transistors", *arXiv:1811.09146v1 [cond-mat.mes-hall]*, Nov. 2018.
- [25] N. Planes, O. Weber, V. Barral, S. Haendler, D. Noblet, D. Croain, M. Bocat, P.-O. Sassoulas, X. Federspiel, A. Cros, A. Bajoulet, E. Richard, B. Dumont, P. Perreau, D. Petit, D. Golanski, C. Fenouillet-Branger, N. Guillot, M. Rafik, V. Huard, S. Puget, X. Montagner, M.-A. Jaud, O. Rozeau, O. Saxod, F. Wacquant, F. Monsieur, D. Barge, L. Pinzelli, M. Mellier, F. Boeuf, F. Arnaud, and M. Haond, "28nm FDSOI technology platform for high-speed low-voltage digital applications", *2012 Symposium on VLSI Technology (VLSIT)*, Honolulu, HI, 2012, pp. 133 - 134. doi: 10.1109/VLSIT.2012.6242497
- [26] R. Wacquez, M. Vinet, M. Pierre, B. Roche, X. Jehl, O. Cueto, J. Verdijin, G. C. Tettamanzi, S. Rogge, V. Deshpande, B. Previtali, C. Vizioz, S. Pauliac-Vaujour, C. Comboroure, N. Bove, O. Faynot, and M. Sanquer, "Single dopant impact on electrical characteristics of NMOSFETs with effective length down to 10nm", *2010 Symposium on VLSI Technology*, Honolulu, 2010, pp. 193 - 194. doi: 10.1109/VLSIT.2010.5556224
- [27] M. Lundstrom, *Fundamentals of nanotransistors (Lessons from Nanoscience: A Lecture Notes Series, Vol. 6)*, Singapore, World Scientific Co. Pte. Ltd., 2018, pp. 143 - 181.
- [28] N. Ma and D. Jena, "Carrier statistics and quantum capacitance effects on mobility extraction in two-dimensional crystal semiconductor field-effect transistors", *2D Materials*, vol. 2, no. 015003, Jan. 2015. doi: 10.1088/2053-1583/2/1/015003
- [29] I. M. Lifshitz, "The energy spectrum of disordered systems", *Advances in Physics*, vol. 13, no. 483, pp. 483 - 536. Oct. 1964. doi: 10.1080/00018736400101061
- [30] A. Gold, J. Serre, and A. Ghazali, "Density of states in a two-dimensional electron gas: Impurity bands and band tails", *Phys. Rev. B*, vol. 37, no. 9, pp. 4589 - 4603, Mar. 1988. doi: 10.1103/PhysRevB.37.4589
- [31] R. M. Jock, S. Shankar, A. M. Tyryshkin, J. He, K. Eng, K. D. Childs, L. A. Tracy, M. P. Lilly, M. S. Carroll, and S. A. Lyon, "Probing band-tail states in silicon metal-oxide-semiconductor heterostructures with electron spin resonance", *Appl. Phys. Lett.*, vol. 100, 023503, Jan. 2012. doi: 10.1063/1.3675862
- [32] H. Bohuslavskyi, S. Barraud, V. Barral, M. Casse, L. Le Guevel, L. Hutin, B. Bertrand, A. Crippa, X. Jehl, G. Pillonnet, A. G. M. Jansen, F. Arnaud, P. Galy, R. Maurand, S. De Franceschi, and M. Vinet, "Cryogenic Characterization of 28-nm FD-SOI Ring Oscillators With Energy Efficiency Optimization", *IEEE Transactions on Electron Devices*, vol. 65, no. 9, pp. 3682-3688, Sept. 2018. doi: 10.1109/TED.2018.2859636
- [33] N. F. Mott and E. A. Davis, *Electronic Processes in Non-crystalline Materials (2nd Edition)*, Oxford, Clarendon Press, 1979, pp. 7 - 62.